

MELLM: Exploring LLM-Powered Micro-Expression Understanding Enhanced by Subtle Motion Perception

Zhengye Zhang[†], Sirui Zhao^{*,†}, Shifeng Liu, Shukang Yin, Xinglong Mao, Tong Xu, *Member, IEEE*, and Enhong Chen^{*}, *Fellow, IEEE*

Abstract—Micro-expressions (MEs) are crucial psychological responses with significant potential for affective computing. However, current automatic micro-expression recognition (MER) research primarily focuses on discrete emotion classification, neglecting a convincing analysis of the subtle dynamic movements and inherent emotional cues. The rapid progress in multimodal large language models (MLLMs), known for their strong multimodal comprehension and language generation abilities, offers new possibilities. MLLMs have shown success in various vision-language tasks, indicating their potential to understand MEs comprehensively, including both fine-grained motion patterns and underlying emotional semantics. Nevertheless, challenges remain due to the subtle intensity and short duration of MEs, as existing MLLMs are not designed to capture such delicate frame-level facial dynamics. In this paper, we propose a novel Micro-Expression Large Language Model (MELLM), which incorporates a subtle facial motion perception strategy with the strong inference capabilities of MLLMs, representing the first exploration of MLLMs in the domain of ME analysis. Specifically, to explicitly guide the MLLM toward motion-sensitive regions, we construct an interpretable motion-enhanced color map by fusing onset-apex optical flow dynamics with the corresponding grayscale onset frame as the model input. Additionally, specialized fine-tuning strategies are incorporated to further enhance the model’s visual perception of MEs. Furthermore, we construct an instruction-description dataset based on Facial Action Coding System (FACS) annotations and emotion labels to train our MELLM. Comprehensive evaluations across multiple benchmark datasets demonstrate that our model exhibits superior robustness and generalization capabilities in ME understanding (MEU). Code is available at <https://github.com/zyzhangUstc/MELLM>.

Index Terms—Multimodal Large Language Models, Micro-expression Understanding

I. INTRODUCTION

MICRO-EXPRESSIONS (MEs) are brief and involuntary facial expressions that occur when individuals attempt to conceal their genuine emotions, revealing underlying feelings despite conscious efforts to suppress them. They hold significant application value in fields such as forensic interrogation, education, and healthcare [1]–[4]. Due to their fleeting

Zhengye Zhang, Sirui Zhao, Tong Xu, and Enhong Chen are with School of Computer Science and Technology, University of Science and Technology of China, Hefei, Anhui 230027, China. E-mail: zhengyezhang@mail.ustc.edu.cn, {siruit, tongxu, cheneh}@ustc.edu.cn

Shifeng Liu, Shukang Yin and Xinglong Mao are with School of Artificial Intelligence and Data Science, University of Science and Technology of China, Hefei, Anhui 230027, China. E-mail: {1sf0619, xjtupanda, maoxl}@mail.ustc.edu.cn

^{*}Corresponding authors, [†]Equally contributed to this work

User

Prompt

Identify the dynamic changes in facial features between two images, recognize action units, and infer the micro-expression being conveyed.



onset apex

Gemini-2.5-pro

Image 1 features a neutral expression with open eyes. Image 2's key difference is isolated AU 43 (eyes closed), lacking significant eyebrow/mouth changes. This suggests a brief state (e.g., disengagement, processing, mild tiredness) without strong emotional indicators.

User

Prompt

Identify the dynamic changes in facial features throughout the video, recognize action units, and infer the micro-expression being conveyed.

Qwen-VL-MAX

The video shows a person with glasses looking at the camera, gradually closing their eyes (likely a natural blink or calm moment). A slight gaze shift suggests altered focus. Without significant changes in other facial features (mouth, eyebrows), this isolated eye closure reflects relaxation or contemplation, not strong emotional cues.



Video

Ground Truth

AUs: Right AU1 + Right AU2 + Right AU12

Micro-expression: Surprise

Fig. 1. An example illustrating the limitation of MLLMs in understanding MEs. In this case, the models fail to recognize expression-related AUs, and therefore cannot infer the ME displayed on the face. (Only key parts of the models’ responses are shown due to length constraints.)

duration (typically less than 0.5 seconds [5]), subtle intensity, and localized muscle movements, improving a model’s ability to perceive these fine-grained facial motions has been a major challenge in automatic micro-expression recognition (MER) [6]. While existing MER algorithms achieve moderate success in discrete emotion classification tasks, they lack explicit and intuitive analysis of the nuanced facial movements and emotional subtleties that MEs convey, thereby limiting their practical applicability and interpretability.

To address these shortcomings, we are inspired by the recent successes of multimodal large language models (MLLMs). These models integrate visual, textual, and sometimes auditory inputs and have demonstrated impressive performance across a wide range of multimodal understanding and generation tasks [7]. In essence, MLLMs reformulate discriminative tasks (such as regression and classification) into text-generation tasks based on powerful large language models (LLMs). Leveraging their robust visual perception, multimodal reasoning,

and language generation capabilities may facilitate a deeper understanding of MEs, encompassing both the subtle motion patterns and their underlying emotional semantics. However, due to the inherently weak and fragmented nature of MEs, existing MLLMs are not well-equipped to capture these delicate frame-level facial dynamics [8]. Our preliminary experiments indicate that state-of-the-art MLLMs often struggle to distinguish between onset and apex frames in ME sequences, frequently perceiving them as nearly identical. Moreover, these models also face challenges in capturing the subtle temporal dynamics essential for accurately interpreting ME videos. As illustrated in Fig. 1, both Gemini-2.5-Pro [9] and Qwen-VL-MAX [10] fail to detect emotion-related facial action details, making it difficult for them to infer the presence of ME.

In affective computing, MLLMs have been explored for recognizing both static and dynamic facial expressions. EmoLA [11] incorporates facial prior experts and Low-Rank Adaptation (LoRA) [12] into a LLM decoder to improve the recognition of static facial emotions and action units (AUs). Emotion-LLaMA [13] integrates both visual and auditory features for video-based emotion recognition. Similarly, EMO-LLaMA [14] leverages facial analysis experts to extract prior facial knowledge and AU-related features, thereby enhancing the model's sensitivity to dynamic facial expressions. However, these models primarily target macro-expressions with pronounced motion and remain less capable of recognizing the subtle motions in MEs. Additionally, they typically use a pre-trained vision encoder to extract prior expression-related features before projecting them into the large model to perform fine-tuning via lightweight adapters such as LoRA. Unfortunately, directly applying a similar framework to the ME task requires a large training dataset to enable the MLLMs to perceive subtle motion, a practically unfeasible requirement due to the scarcity of ME samples caused by the stringent conditions necessary for elicitation and annotation.

Capitalizing on the powerful visual understanding capabilities of MLLMs, we propose leveraging optical flow as a mechanism to translate subtle facial motions into a form interpretable by MLLMs. Specifically, optical flow encodes pixel-level motion between frames, making it particularly effective for capturing the nuanced, localized movements characteristic of MEs. Through chromatic encoding (hue for motion direction) and luminance intensity (brightness for magnitude), we generate spatially grounded motion representations that align with MLLMs' pretrained visual understanding. By superimposing these motion maps onto facial images, we create hybrid inputs that transform imperceptible facial dynamics into visually interpretable cues.

Building upon this idea, we introduce the Micro-Expression Large Language Model (MELLM) based on Qwen2.5-VL [15]. MELLM incorporates optical flow-guided inputs and is fine-tuned using LoRA strategies to enhance its generalization on small-scale ME datasets. This design enables MELLM to reason about both activated facial AUs and the emotional semantics of MEs despite the limited training data and the subtlety of temporal facial cues.

Our main contributions are as follows:

- We explore the feasibility of applying MLLMs to the task

of ME understanding (MEU).

- We introduce a ME Motion-enhanced Color Mapping (MMC-Mapping) method, which explicitly enhances the subtle motion-sensitive regions by fusing optical flow dynamics with the corresponding grayscale frame.
- We propose a Flow-Guided Micro-Expression Understanding (FGMU) strategy, which establishes an alignment between optical flow features and AU annotations, thereby enabling interpretable AU identification and robust ME inference. Building upon this strategy, we construct a MEU instruction dataset that supports fine-grained understanding of MEs.
- We propose MELLM, the first LLM-based framework tailored for MEU, capable of inferring both AUs and expression categories.

The remainder of this paper is organized as follows. Section II reviews related work from three perspectives: MER methods, MLLMs, and emotion recognition LLMs. Section III introduces our proposed approach, including the task definition, data construction method, and model framework. Section IV presents the experimental settings and result analysis. Finally, conclusions and future directions are discussed in Section V.

II. RELATED WORK

A. Micro-expression Recognition

As a crucial pathway for understanding human emotional behavior, automatic MER has long attracted significant research interest in the field of Affective Computing. A central challenge of MER lies in enhancing a model's sensitivity to the subtle and localized facial movements characteristic of MEs.

In the early stages of MER research, many studies relied on handcrafted visual descriptors to extract appearance- or geometry-based features. Representative examples include LBP-TOP [16], 3DHOG [17], MDMO [18], and Bi-WOOF [19], which were typically fed into supervised classifiers such as Support Vector Machines (SVMs) [20] to predict target emotions. While these methods offer geometric invariance and low computational cost, they fundamentally struggle to capture the subtle and complex spatiotemporal patterns inherent in MEs. With the rapid progress of deep learning, powerful visual representation models such as Convolutional Neural Networks (CNNs), Graph Convolutional Networks (GCNs), and Vision Transformers (ViTs) have been introduced to MER tasks, aiming to extract expressive spatiotemporal features of ME dynamics [21]–[25]. In addition to using raw apex frames or image sequences as input [26]–[28], a popular alternative is to compute the optical flow between frames in a ME sequence, especially the onset and apex frames [29]–[32]. This approach helps suppress identity-related biases while preserving crucial motion cues. However, although optical flow reduces the influence of facial identity, it also removes useful structural priors from the facial appearance. Moreover, due to the limited size of available ME datasets, deep models are prone to overfitting and often exhibit poor generalization performance. To overcome these limitations, recent advances have explored contrastive learning and self-supervised learning [33]–[36],

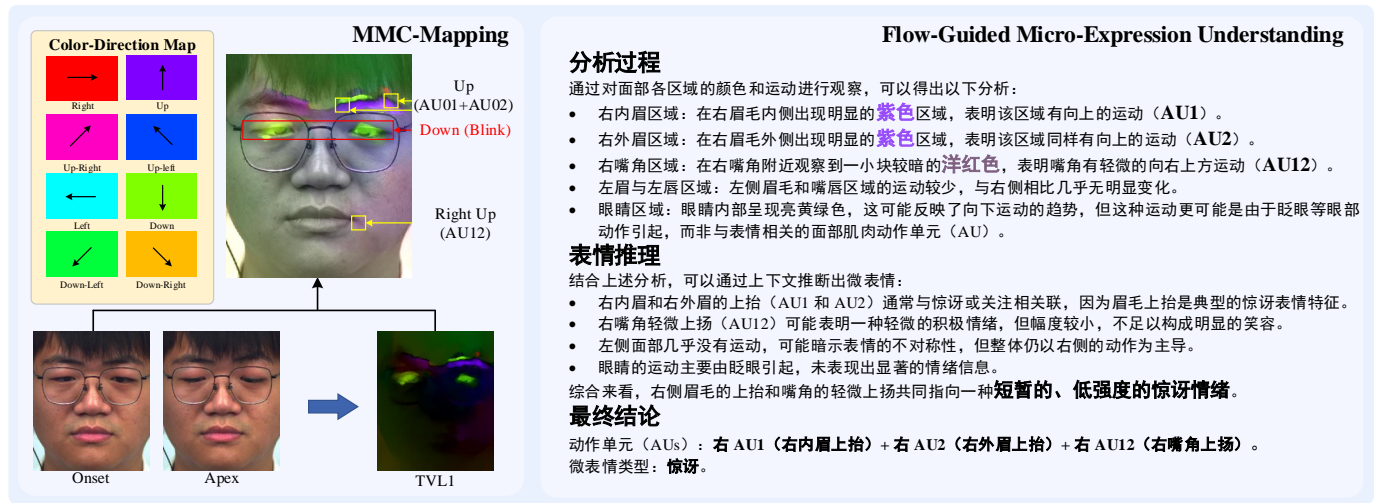


Fig. 2. An example of the construction and annotation process of the instruction-following MEU dataset. The left part illustrates the generation of an MMC-Map, while the right part presents its annotation based on the FGMU strategy.

which aim to enhance representation quality while minimizing dependence on manual annotations.

Despite the improved performance these methods have achieved in discrete emotion classification tasks, they still lack the ability to achieve fine-grained understanding of facial dynamics and the emotional subtleties conveyed by MEs. This limitation significantly hinders their practical utility in real-world applications requiring interpretable affective reasoning. Therefore, we propose incorporating MLLMs into MER, leveraging their advanced reasoning abilities to construct a comprehensive Micro-Expression Understanding System.

B. Multimodal Large Language Models

In recent years, MLLMs have evolved as prominent tools for various domains and downstream tasks [7]. Built upon large parameter sizes and large-scale training, MLLMs exhibit unprecedented perception [37] and reasoning [38], [39] capabilities. These powerful models open up new possibilities and inspire new research paradigms for traditional vision or multi-modal tasks. For instance, Shikra [40] explores visual-grounded dialogues via numeral representation of object coordinates. LISA [41] leverages the reasoning capabilities of LLM and develops a framework for reasoning-based segmentation, which enables a more flexible and advanced form of referring image segmentation.

In this work, we leverage MLLMs' outstanding perception and semantic understanding abilities for a more comprehensive and fine-grained understanding of MEs. Different from previous specialist methods [42], [43], we explore the possibility of adopting a multi-step reasoning process, which aligns with the analysis procedure of human experts and enables a more interpretable method for automatic MEU.

C. Emotion Recognition Large Language Models

Recent years have seen a surge in applying LLMs and MLLMs to emotion recognition tasks. Text-only models such as EmoLLMs [44] have leveraged instruction tuning with

large-scale affective datasets to improve performance across sentiment classification and regression tasks, achieving results competitive with models like ChatGPT and GPT-4. However, these models are limited to linguistic inputs and overlook visual or temporal affective cues.

To extend LLMs towards multimodal emotion understanding, several works have introduced MLLMs by incorporating various combinations of image, video, and audio modalities. For instance, ExpLLM [45] proposes chain-of-thought reasoning based on AUs, enabling interpretable expression recognition. EmoLA [11] and EMO-LLaMA [14] improve facial affective behavior analysis by incorporating prior knowledge of facial structure, leading to enhanced recognition of fine-grained emotions. Furthermore, Emotion-LLaMA [13] integrates audio, visual, and textual information with modality-specific encoders and achieves state-of-the-art results on multimodal emotion benchmarks. While these models demonstrate strong performance on macro-expression and general affective tasks, their ability to capture the subtle and transient nature of MEs remains limited due to insufficient temporal granularity and domain-specific understanding.

III. METHODOLOGY

In this section, we provide a detailed introduction to our technical pipeline, including the task definition, an overview of the framework, and the core components of our model.

A. Task Definition

Different from the traditional MER task, which focuses solely on classifying MEs into discrete emotional categories, we propose an extended formulation of the task, termed Micro-Expression Understanding (MEU). This formulation goes beyond simple classification, aiming to provide a comprehensive and interpretable understanding of the observed facial subtle behavior. Specifically, our MEU task mainly comprises three key components:

- Facial Action Analysis: Analyzing the subtle, transient changes across different facial regions and identifying, as well as potentially quantifying, the activation of relevant AUs corresponding to these movements.
- Inferential Reasoning: Constructing a logical inference process based on the observed facial dynamics and AU activations to infer the underlying expressive state.
- Result Conclusion: Providing explicit outputs in terms of the identified AUs and the corresponding ME category.

Compared to conventional MER, MEU aims to offer an intuitive, justifiable, and transparent interpretation of MEs. By incorporating detailed facial analysis and explicit reasoning processes, MEU enhances model interpretability and generalization capabilities, thereby fostering greater trustworthiness and enabling more robust and versatile applications in domains requiring nuanced understanding of human affective states.

B. Framework Overview

To advance MEU, we propose a novel framework that incorporates facial motion-aware enhancement with MLLM. Central to this framework is the ME Motion-enhanced Color Mapping (MMC-Mapping) module, which improves the visibility of subtle facial dynamics by mapping the direction and magnitude of motion cues derived from optical flow into the color-enhanced facial representation. Building upon the MMC-Mapping module, we further devise the Flow-Guided Micro-Expression Understanding (FGMU) strategy, which aligns optical flow patterns with AU annotations to enable interpretable AU identification and ME inference. Furthermore, we introduce MELLM, a LoRA-tuned MLLM framework that progressively reasons from ME motion analysis to expression classification, utilizing motion-enhanced inputs and structured prompts. Together, these components constitute a unified and effective MEU pipeline, bridging fine-grained motion cues and high-level affective understanding.

C. ME Motion-enhanced Color Mapping

Due to the subtle and concealed nature of MEs, it is difficult to accurately capture the specific facial AUs or expressions corresponding to minor facial changes from a single frame. Therefore, it is often necessary to repeatedly compare the onset and apex frames, or to closely examine the entire ME video in detail. In addition, MLLMs possess limited dynamic perception abilities for subtle motion, and it is particularly challenging to train these models to directly recognize MEs when working with small-scale datasets.

To address this issue, the MMC-Mapping module is proposed to improve the visibility of subtle facial dynamics. Specifically, the TLV1 optical flow is computed between the onset and apex frames of a ME sequence, and local optical flow in the nose-tip region is subtracted to compensate for head movement. Then, the direction of the optical flow is mapped to the hue component in the HSV color space, and the flow magnitude is mapped to the value (brightness). Finally, the filtered optical flow is superimposed onto a grayscale version of the onset frame to ensure the correspondence between the optical flow and the face region. As shown on the left side of

Fig. 2, we illustrate the process of MMC-Map generation and provide a Color-Direction Mapping table. In our method, eight primary motion directions are considered, where rightward motion is represented in red, and the other directions are assigned colors according to the hue wheel.

D. Flow-Guided Micro-Expression Understanding

To bridge the gap between low-level motion features and high-level emotional interpretations, we propose FGMU—a structured analysis strategy that utilizes optical flow for MEU.

The FGMU strategy consists of three sequential stages: (1) Motion Analysis and AU Recognition: FGMU requires models to systematically examine color patterns and motion intensity in semantically important facial regions. By interpreting these localized motion flows, the models identify active AUs that correspond to specific facial muscle movements. (2) Expression Inference: Once the active AUs are recognized, the models integrate them with the overall motion context to infer the most likely ME category. This inference is grounded in established relationships between AUs and emotional expressions, ensuring semantic validity and physiological plausibility. (3) Conclusion: Finally, the models produce a concise and interpretable description that summarizes the recognized AUs and the inferred expression category.

E. Instruction-following MEU Dataset Construction

Guided by the FGMU strategy, we construct an instruction-following MEU dataset based on the original annotations from the DFME dataset [46]. The construction process is as follows: First, we analyze the color patches and their corresponding motion directions according to the Color-Direction Map. For key facial regions such as the eyebrows, eyelids, cheeks, mouth, and chin, we examine the color, motion direction, and motion intensity of each patch to determine whether it corresponds to an AU, based on the DFME annotations. If a region exhibits motion consistent with the labeled AUs, we record the patch's color, motion direction, motion intensity, and the associated AU identifier. Color patches outside facial regions or those linked to AUs that are less relevant to MEs (e.g., blinking) are noted with their color, motion direction, and intensity, but without an AU label. Subsequently, based on the distribution of AUs and the contextual pattern of facial motion, we infer the corresponding ME. The final result includes the identified AUs with their descriptions, as well as the inferred ME label. To facilitate this process, we initially employed Gemini-2.5-Pro [9] to generate annotations according to the FGMU strategy, which were then manually proofread and refined for accuracy and internal logic.

As illustrated by the annotation example on the right side of Fig. 2, the FGMU strategy ensures a consistent correspondence between AUs and the MMC-Maps. Additionally, it establishes a clear association between AUs and expression categories, forming a complete reasoning process that progresses from optical flow features and facial region information, through AU identification, to ME inference.

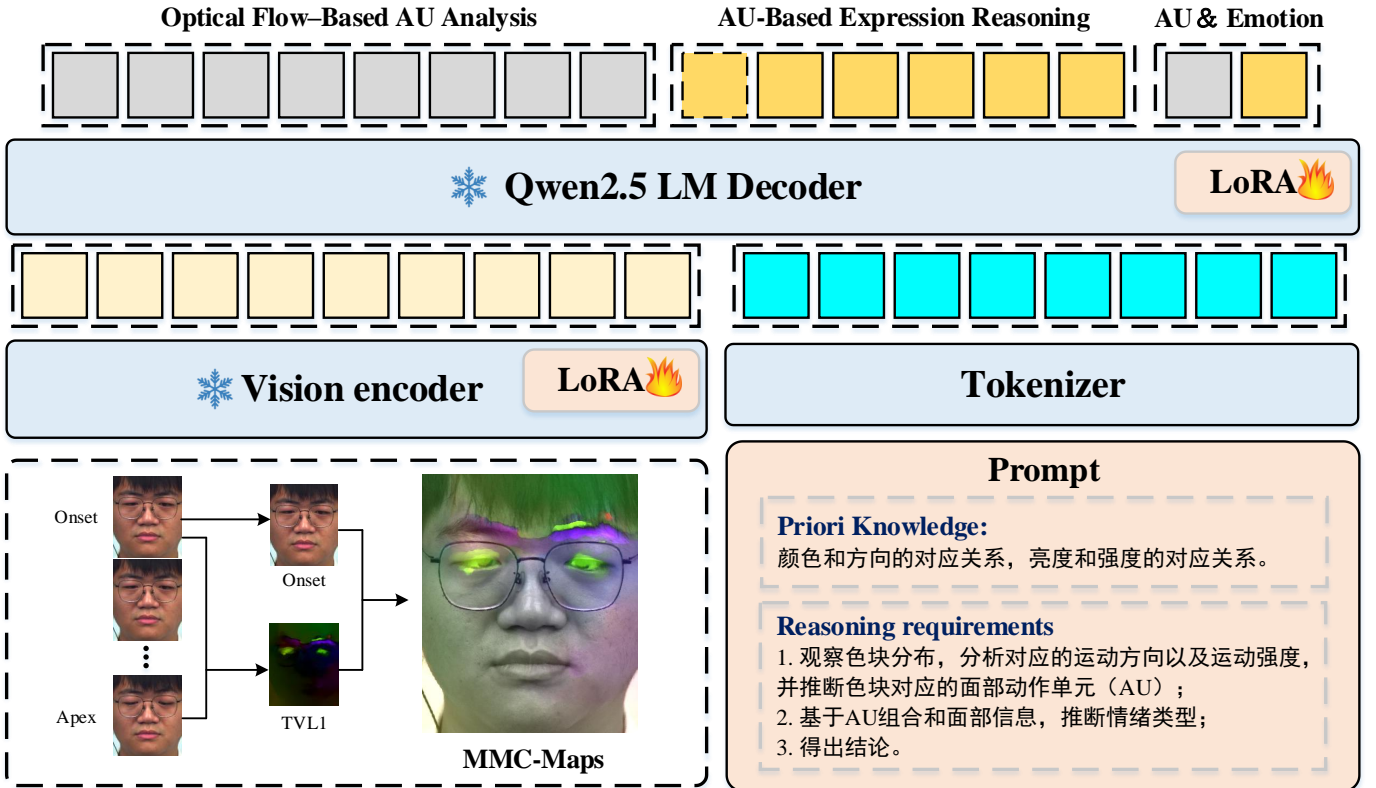


Fig. 3. The pipeline of proposed MELLM. The visual input consists of MMC-Maps, while the textual input includes prior knowledge and reasoning requirements. The MELLM is built upon the Qwen2.5-VL architecture, with both the vision encoder and LM decoder fine-tuned using LoRA.

F. MELLM: An Fine-tuned MLLM for MEU

As illustrated in Fig. 3, our method adopts Qwen2.5-VL-7B as the base MLLM. To enable efficient fine-tuning, we integrate LoRA Adapter modules into both the vision encoder and the Qwen2.5 Language Model (LM) decoder. This lightweight, parameter-efficient tuning strategy improves the model's sensitivity to subtle ME details while maintaining a relatively small number of trainable parameters. The model takes MMC-Maps as input, which are first encoded into visual tokens via the vision encoder. These visual tokens are then combined with text tokens generated from the designed prompt, and together they are fed into the LM decoder for inference. Inspired by the approach proposed in [13], we employ a mixed training paradigm that jointly optimizes both MEU and MER tasks during training. In the MER task, the model is required to output only the predicted emotion category, without generating explanatory text. This multi-task learning strategy enables the model to leverage complementary information from both tasks, thereby enhancing its performance on the MEU task.

The prompt design consists of two parts. The first part introduces prior knowledge about the correspondence between color and direction and between brightness and intensity, serving as a reference for the model to correctly interpret the MMC-Maps. The second part defines a step-by-step reasoning instruction, guiding the model to: (1) observe the distribution of color patches, analyze their motion directions and intensities, and infer the corresponding AUs associated with these motion patterns; (2) predict the type of ME by combining

the identified AU patterns with facial information; and (3) conclude the final ME inference result.

The model's output is structured into three components: Optical Flow-Based AU Analysis, AU-Based Expression Reasoning, and the Final Conclusion. This framework not only enables a progressive, interpretable reasoning process from optical flow analysis to AU identification and ME inference, but also ensures the clarity, structure, and explainability of the model's outputs.

IV. EXPERIMENTS

In this section, we present the experimental settings, introduce the datasets along with the evaluation protocols and metrics, and conduct a comprehensive analysis of MELLM's performance, concluding with a case study.

A. Experimental Settings

We fine-tune our multi-modal model based on Qwen2.5-VL-7B, utilizing LoRA for parameter-efficient adaptation. LoRA is applied to both the vision encoder and the language model decoder, with the rank and alpha set to 64. We employ AdamW optimization with a learning rate of 1e-4, coupled with a cosine learning rate scheduler. The model is fine-tuned for 1,200 steps on two NVIDIA A100 GPUs.

B. Datasets

We conduct training using the DFME dataset, which comprises 7,526 ME samples collected from 656 participants.

From this dataset, we select 4,793 samples and annotate them in detail following the FGMI strategy, with the initial annotation generated by Gemini-2.5-Pro and subsequently refined through manual proofreading. These annotated samples constitute the Instruction-following MEU Dataset, which encompasses instances of the seven basic emotions (happiness, disgust, contempt, surprise, fear, anger, and sadness) and are utilized for instruction tuning. For evaluation, we assess our model on the DFME TestA set (474 samples) and TestB set (299 samples).

To further evaluate the generalization ability of our model, we perform zero-shot testing on two additional ME datasets: CASME II [47] and CAS(ME)³ [48], which are not seen during training.

CASME II comprises 247 ME clips collected from 26 subjects. It features a high temporal resolution of 200 fps and a facial region resolution of 280×340 pixels, allowing for detailed analysis of subtle facial dynamics. For consistency with the emotion categories used in DFME, we select samples corresponding to five emotions: happiness, sadness, fear, surprise, and disgust.

CAS(ME)³ is segmented into Part A and Part C, each based on distinct emotion elicitation methods. Our study primarily focuses on Part A, which includes 943 ME samples. To maintain alignment with DFME, we select samples from six emotion categories: happiness, sadness, fear, surprise, disgust, and anger.

C. Evaluation Protocol and Metrics

During inference, we extract the predicted emotion category from the conclusion section of the model-generated text and use it as the final output for evaluation. This textual prediction is then compared against the ground-truth label to compute quantitative metrics. Following the evaluation protocols in [46], we evaluate our model using Accuracy (ACC), Unweighted F1-score (UF1), and Unweighted Average Recall (UAR), where UF1 and UAR are crucial for a balanced evaluation across emotion categories given the common class imbalance in ME datasets.

ACC measures the overall proportion of correctly predicted samples across all classes:

$$ACC = \frac{\sum_{i=1}^C TP_i}{\sum_{i=1}^C N_i} \quad (1)$$

where TP_i denotes the number of true positives in class i , N_i is the total number of samples in class i , and C is the total number of classes.

UAR represents the unweighted average recall, calculated as the mean of the recall values for each class:

$$UAR = \frac{1}{C} \sum_{i=1}^C \frac{TP_i}{TP_i + FN_i} \quad (2)$$

where FN_i is the number of false negatives for class i .

UF1 refers to the unweighted average F1-score, which is the mean of the F1-scores computed independently for each class, without accounting for class frequency:

TABLE I
EXPERIMENTAL RESULTS COMPARED TO GENERAL MER METHODS ON DFME DATASET (TESTA & TESTB)

MER Methods	Test Set	UF1	UAR	ACC
FearRef [42]	TestA	0.3410	0.3686	0.5084
Wang et al. [43]		0.4067	0.4074	0.4641
He et al. [43]		0.4123	0.421	0.4873
MELLM(ours)		0.3578	0.3731	0.4641
FearRef [42]	TestB	0.2875	0.3228	0.3645
Wang et al. [43]		0.3534	0.3661	0.3813
He et al. [43]		0.4016	0.4008	0.4147
MELLM(ours)		0.3162	0.3424	0.3712

$$UF1 = \frac{1}{C} \sum_{i=1}^C \frac{2 \cdot P_i \cdot R_i}{P_i + R_i} \quad (3)$$

where $P_i = \frac{TP_i}{TP_i + FP_i}$ is the precision and $R_i = \frac{TP_i}{TP_i + FN_i}$ is the recall for class i , and FP_i denotes the number of false positives in class i .

D. Experiment Results Analysis

Comparison with general MER Methods. As shown in TABLE I, our method surpasses the FearRef [42] baseline in terms of UF1 and UAR, which highlights the advantage of jointly modeling AU inference and emotion reasoning. Nevertheless, it still lags behind the specialized ME classifiers [43], which benefit from end-to-end optimization and targeted regularization. Unlike traditional expert models that focus solely on ME classification and risk overfitting on limited datasets, MELLM incorporates a reasoning pipeline that performs AU analysis and emotion inference based on optical flow. This design facilitates richer contextual understanding, though it may lead to a slight trade-off in classification performance. Future work will focus on refining our approach to enhance classification performance and narrow this gap, while preserving the benefits of our reasoning framework.

Comparison with Other MLLMs. We conducted a comparative analysis against Qwen2.5-VL-7B (without finetuning), Qwen-VL-Max [10], and Gemini-2.5-Pro [9]. These MLLMs were evaluated on multiple ME datasets, including CASME II, CAS(ME)³, and two test sets from the DFME benchmark. To ensure a fair comparison, we explicitly constrained the emotion category options in the prompt when evaluating other MLLMs, guiding them to choose from a fixed set of predefined emotion labels consistent with the target dataset. When provided with ME video clips or paired onset and apex frames, these MLLMs often failed to capture the subtle facial movements characteristic of MEs, frequently defaulting to a "neutral" classification. In contrast, when MMC-Maps were introduced together with prompts embedding prior knowledge—specifically, the correspondence between color and direction, and between intensity and brightness—the MLLMs demonstrated improved performance, particularly Gemini-2.5-Pro, although their overall effectiveness remained constrained.

TABLE II
COMPARISON WITH OTHER MLLMs

Models	Class	Dataset	UF1	UAR	ACC
Qwen2.5-VL-7B	5	CASME II	0.0782	0.1886	0.1628
Qwen-VL-Max			0.1039	0.1062	0.1008
Gemini-2.5-Pro			<u>0.2717</u>	<u>0.2633</u>	<u>0.3023</u>
MELLM(ours)			0.4849	0.5337	0.6434
Qwen2.5-VL-7B	6	CAS(ME) ³	0.1079	<u>0.1787</u>	<u>0.2507</u>
Qwen-VL-Max			0.1623	0.1698	0.1905
Gemini-2.5-Pro			<u>0.1767</u>	0.1663	0.2092
MELLM(ours)			0.2908	0.2948	0.4226
Qwen2.5-VL-7B	7	DFME TestA	0.0794	0.1495	0.2046
Qwen-VL-Max			0.1788	0.1883	0.2025
Gemini-2.5-Pro			<u>0.3056</u>	<u>0.3363</u>	<u>0.3481</u>
MELLM(ours)			0.3578	0.3731	0.4641
Qwen2.5-VL-7B	7	DFME TestB	0.0737	0.1499	0.1605
Qwen-VL-Max			0.1550	0.1677	0.1672
Gemini-2.5-Pro			<u>0.2665</u>	<u>0.2818</u>	<u>0.2843</u>
MELLM(ours)			0.3162	0.3424	0.3712

TABLE III

COMPARISON BETWEEN SINGLE-TASK AND MULTI-TASK TRAINING PERFORMANCE. MELLM* DENOTES THE MODEL TRAINED SOLELY ON THE MEU TASK, WHILE MELLM REPRESENTS THE MODEL TRAINED WITH A MIXED MEU AND MER PARADIGM.

Models	Dataset	UF1	UAR	ACC
MELLM*	CASME II	0.4026	0.3878	0.5504
MELLM		0.4849	0.5337	0.6434
MELLM*	CAS(ME) ³	0.2774	0.2776	0.3725
MELLM		0.2908	0.2948	0.4226
MELLM*	DFME TestA	0.3399	0.3592	0.4346
MELLM		0.3578	0.3731	0.4641
MELLM*	DFME TestB	0.3057	0.3171	0.3445
MELLM		0.3162	0.3424	0.3712

As shown in TABLE II, our method consistently achieves the highest scores in UF1, UAR, and ACC across all evaluation datasets, demonstrating its robustness and superior performance. Remarkably, MELLM achieves superior results on the CASME II and CAS(ME)³ datasets in a zero-shot setting, underscoring its strong generalization capability.

Effectiveness of multi-task training. To improve the model's performance on the MEU task, we adopt a multi-task training strategy that jointly optimizes both MEU and MER objectives. Under this setting, the model learns from the explanatory signals of MEU while also being supervised by the emotion classification task in MER. As shown in TABLE III, the model trained with this mixed paradigm consistently outperforms the single-task version across all datasets and evaluation metrics. This performance gain indicates that the auxiliary supervision from the MER task provides complementary information, enabling the model to learn more robust and discriminative features for MEU.

E. Case Study

Figure 4 presents a comparison of MELLM, Qwen2.5-VL-7B, and Qwen-VL-Max through two illustrative examples on the MEU task. In the first example, our MELLM accurately detects color and motion patterns around the cheeks and mouth corners, leading to the correct recognition of AU06 and AU12 and the inference of happiness. Similarly, in the second example, MELLM captures facial dynamics in the eyebrow and chin regions, correctly identifying AU04 and AU17 and inferring disgust.

However, both Qwen2.5-VL-7B and Qwen-VL-Max fail in these cases, highlighting their limitations in comparison to MELLM. It is evident that both MLLMs exhibit weaker capabilities in perceiving regional color, making them prone to hallucinations. Furthermore, their performance in AU recognition and emotional reasoning is significantly limited. Notably, Qwen2.5-VL-7B demonstrates a clear lack of knowledge related to AUs. In contrast, MELLM effectively perceives facial color distribution, accurately identifies the corresponding AUs, and successfully infers the correct ME.

V. CONCLUSION

In this paper, we proposed MELLM, a novel micro-expression large language model by incorporating subtle motion perception strategy and the strong inference ability of MLLMs. Specifically, to explicitly guide the MLLM toward motion-sensitive regions, we constructed an interpretable motion-enhanced color map by fusing onset-apex optical flow dynamics with the corresponding grayscale onset frame as the model input. Additionally, specialized fine-tuning strategies are incorporated to further enhance the model's visual perception of MEs. Furthermore, we constructed an instruction-following dataset based on FACS annotations and emotion labels to train our MELLM. Comprehensive evaluations across multiple benchmark datasets demonstrated that our model exhibits superior robustness and generalization capabilities in MEU. Future work will concentrate on improving AU recognition and classification accuracy.

ACKNOWLEDGMENTS

This work was supported by the National Natural Science Foundation of China (Grant No. 61727809, 62406264).

REFERENCES

- [1] P. Ekman, *Telling Lies: Clues to Deceit in the Marketplace, Politics, and Marriage (Revised Edition)*. W. W. Norton & Company, 2009.
- [2] S. Weinberger, “Airport security: Intent to deceive?” *Nature*, vol. 465, no. 7297, pp. 412–416, 2010.
- [3] L. Hunter, L. Roland, and A. Ferozpurji, “Emotional expression processing and depressive symptomatology: Eye-tracking reveals differential importance of lower and middle facial areas of interest,” *Depression Research and Treatment*, vol. 2020, no. 1, p. 1049851, 2020.
- [4] M. P. Haselhuhn, E. M. Wong, M. E. Ormiston, M. E. Inesi, and A. D. Galinsky, “Negotiating face-to-face: Men's facial structure predicts negotiation performance,” *The Leadership Quarterly*, vol. 25, no. 5, pp. 835–845, 2014.
- [5] W.-J. Yan, Q. Wu, J. Liang, Y.-H. Chen, and X. Fu, “How fast are the leaked facial expressions: The duration of micro-expressions,” *Journal of nonverbal behavior*, vol. 37, pp. 217–230, 2013.
- [6] P. Ekman and W. V. Friesen, “Nonverbal leakage and clues to deception,” *Psychiatry*, vol. 32, no. 1, pp. 88–106, 1969.



User

这是一个人脸图像，叠加了微表情的可视化光流图。在此图像中，每个面部区域的颜色表示运动的方向，亮度表示运动的幅度。颜色到方向的映射如下：

向上：紫色；右上：品红色/粉红色；向右：红色；右下：橙黄色；向下：黄绿色；左下：绿色；向左：青色；左上：蓝色。

你需要按以下步骤进行分析：

视觉检查：仔细观察颜色块在不同面部区域的分布。排除整体头部运动和亮度较低（运动较弱）的区域。仅关注明显的局部运动单元。识别每个关键区域的颜色、相应的运动方向和运动强度。并基于特定面部区域的运动方向和幅度，推断图像中涉及的面部动作单元（AUs）。

表情推理：结合上下文信息，并根据识别出的面部动作单元（AUs）及其组合，推理出人脸所表达的微表情。

最终结论：请总结分析结果，明确列出推断出的面部动作单元（AUs）以及最终推断的微表情。

（微表情归类为以下七种情绪之一：开心、悲伤、害怕、惊讶、厌恶、轻蔑或生气。）



分析过程

1. 视觉检查：

- 脸颊/眼下区域：双眼下方及延伸至脸颊的部分可见显著运动。左侧呈现蓝/青色斑块（左上/左方运动），右侧呈现粉/洋红色斑块（右上运动）。亮度表明运动强度适中。
- 嘴角区域：两侧嘴角均显示出明显运动。左侧嘴角呈现蓝/紫色斑块（左上/上方运动），右侧嘴角呈现粉/洋红色斑块（右上运动）。亮度同样表明运动强度适中。
- 其他区域：额头、眉毛或下巴未检测到显著运动。

2. 动作单元（AU）推断：

- 眼下及脸颊区域的向上和向外运动（左侧为左上，右侧为右上）符合**AU06（颤大肌收缩）**的特征。
- 嘴角的向上和向外拉伸运动（左侧为左上，右侧为右上）符合**AU12（嘴角提升）**的特征。

表情推理

通过上下文分析可知：

- AU06（颤大肌收缩）通常与眼周皱纹相关联，可能出现在微笑或愉悦的情绪中，但也可能与其他负面情绪如痛苦或不适有关。

- AU12（嘴角提升）是典型的微笑标志，常见于开心或满足的情感表达。

结合这两个动作单元，可以推测该表情并非单纯的痛苦或不适，而是更倾向于一种积极的情绪——即“开心”。因此，综合判断该微表情为“开心”。

最终结论

图像中存在的动作单元（AUs）为：AU06（颤大肌收缩）+ AU12（嘴角提升）。所表现出的微表情类型为：“开心”。

MELLM

视觉检查

- 额头区域：颜色：蓝色；运动方向：左上；运动强度：中等；推断的面部动作单元（AUs）：眉下拉（AU45）。
- 眼睛周围区域：上眼睑区域：紫色；运动方向：向上；运动强度：弱。
- 下眼睑区域：绿色；运动方向：向下；运动强度：中等；推断的面部动作单元（AUs）：皱眉（AU6）。
- 鼻子区域：颜色：白色；运动方向：无明显运动；运动强度：弱；推断的面部动作单元（AUs）：无。
- 脸颊区域：左侧脸颊：青色；运动方向：向左；运动强度：弱；右侧脸颊：红色；运动方向：向右；运动强度：中等；推断的面部动作单元（AUs）：面颊肌收缩（AU10）。
- 下巴区域：颜色：黄绿色；运动方向：向下；运动强度：强；推断的面部动作单元（AUs）：下巴下降（AU12）。

表情推理

结合上述分析，可以推断出以下面部动作单元（AUs）的组合：眉下拉（AU45）；皱眉（AU6）；面颊肌收缩（AU10）；下巴下降（AU12）。

这些AUs组合在一起，通常与轻微的惊讶或困惑的表情相关联。因此，最终推断的微表情为惊讶。

Qwen2.5-VL-7B

视觉检查

仔细观察颜色块在不同面部区域的分布，排除整体头部运动和亮度较低（运动较弱）的区域。仅关注明显的局部运动单元。

- 眼睛区域：颜色：紫色、蓝色；运动方向：向上、左上；运动强度：中等。
- 眉毛区域：颜色：紫色、蓝色；运动方向：向上、左上；运动强度：中等。
- 鼻子区域：颜色：黄绿色；运动方向：向下；运动强度：中等。
- 嘴巴区域：颜色：红色、橙黄色；运动方向：向右、右下；运动强度：较强。
- 脸颊区域：颜色：红色、橙黄色；运动方向：向右、右下；运动强度：较强。

表情推理

结合上下文信息，并根据识别出的面部动作单元（AUs）及其组合，推理出人脸所表达的微表情。

- 眼睛区域：向上和左上的运动可能表示眉毛抬起的动作。

- 眉毛区域：向上和左上的运动可能表示眉毛抬起的动作。

- 鼻子区域：向下的运动可能表示鼻子皱起的动作。

- 嘴巴区域：向右和右下的运动可能表示嘴角向下的动作。

- 脸颊区域：向右和右下的运动可能表示脸颊收缩的动作。

最终结论

总结分析结果，明确列出推断出的面部动作单元（AUs）以及最终推断的微表情。

面部动作单元（AUs）：AU1：眉毛抬起；AU6：下眼睑抬高；AU9：鼻子皱起；AU12：嘴角向下的动作；AU17：嘴唇紧闭

最终推断的微表情：根据上述面部动作单元的组合，可以推断出这张图像中的微表情是“悲伤”。

Qwen-VL-MAX



分析过程

1. 视觉检查：

- 肩部区域：双眉上方可见显著的色块，表明有强烈的运动。具体来说，在观察者的左侧有一个明亮的黄色/橙色斑块，显示眉毛向下并向右移动；在观察者的右侧有一个明亮的绿色斑块，显示眉毛向下并向左移动。两者结合表明眉毛被向下拉，并可能稍微向内聚拢。
- 下巴区域：在唇下方延伸至下巴的位置，出现了一块明显的紫色斑块。紫色对应于向上的运动。

2. 动作单元（AU）推断：

- 眉毛向下并向内移动直接对应于AU04（眉头向下收紧）。
- 下巴区域的向上运动对应于AU17（下巴上抬）。

表情推理

通过上下文分析，可以推断出以下内容：

- AU04（眉头向下收紧）的激活通常与负面情绪相关，例如愤怒、困惑或专注。然而，结合**AU17（下巴上抬）**，这种组合更倾向于表达一种强烈的厌恶感。
- AU17（下巴上抬）通常表现为下巴抬起，下唇微翘，这在表达拒绝或轻蔑时较为常见。当它与**AU04**同时出现时，进一步强化了对某种刺激的反感或不适的情绪。

综合来看，这两种动作单元的协同作用强烈指向一种典型的厌恶情绪。

最终结论

动作单元（AUs）：AU04（眉头向下收紧）+ AU17（下巴上抬）。微表情类型：厌恶

MELLM

视觉检查

- 上眼睑区域：颜色：紫色；运动方向：向上；运动强度：中等；推断的面部动作单元（AUs）：皱眉（AU45）。
- 下眼睑区域：颜色：黄绿色；运动方向：向下；运动强度：中等；推断的面部动作单元（AUs）：闭眼（AU43）。
- 鼻翼区域：颜色：红色；运动方向：向右；运动强度：强；推断的面部动作单元（AUs）：鼻翼收缩（AU4）。
- 脸颊区域：颜色：橙黄色；运动方向：右下；运动强度：强；推断的面部动作单元（AUs）：颊肌收缩（AU6）。
- 下巴区域：颜色：青色；运动方向：向左；运动强度：弱；推断的面部动作单元（AUs）：无明显运动。

表情推理

结合上述分析，可以推断出以下微表情：

- 皱眉（AU45）：上眼睑区域的紫色表示向上运动。
- 闭眼（AU43）：下眼睑区域的黄绿色表示向下运动。

- 鼻翼收缩（AU4）：鼻翼区域的红色表示向右运动。

- 颊肌收缩（AU6）：脸颊区域的橙黄色表示右下运动。

综合这些面部动作单元，可以推测出该人脸所表达的微表情为惊讶。惊讶通常伴随着眉毛上扬、眼睛睁大、鼻翼收缩和脸颊肌肉紧张的动作。

Qwen2.5-VL-7B

视觉检查

额头区域：颜色：紫色和黄绿色；运动方向：向上（紫色）和向下（黄绿色）；运动强度：中等。

眉毛区域：颜色：品红色/粉红色和青色；运动方向：右上（品红色/粉红色）和左上（青色）；运动强度：中等。

眼睛区域：颜色：红色和橙黄色；运动方向：向右（红色）和右下（橙黄色）；运动强度：中等。

鼻子区域：颜色：黄绿色；运动方向：向下（黄绿色）；运动强度：中等。

嘴巴区域：颜色：紫色和青色；运动方向：向上（紫色）和左上（青色）；运动强度：中等。

识别面部动作单元（AUs）

额头区域：AU1（皱眉）；眉毛区域：AU2（扬眉）；眼睛区域：AU6（闭眼）；鼻子区域：AU9（鼻翼扩张）；嘴巴区域：AU12（嘴角上扬）。

表情推理

结合上下文信息和识别出的面部动作单元（AUs），可以推断出以下微表情：

开心：嘴角上扬（AU12）；惊讶：扬眉（AU2）。

最终结论

根据分析结果，推断出的面部动作单元（AUs）包括：AU1（皱眉）；AU2（扬眉）；AU6（闭眼）；AU9（鼻翼扩张）；AU12（嘴角上扬）。

最终推断的微表情为：惊讶。

Qwen-VL-MAX

Fig. 4. Examples comparing MELLM with Qwen2.5-VL-7B and Qwen-VL-Max in MEU. Correct predictions are highlighted with a green background, while incorrect ones are highlighted in red.

[7] S. Yin, C. Fu, S. Zhao, K. Li, X. Sun, T. Xu, and E. Chen, "A survey on multimodal large language models," *National Science Review*, vol. 11, no. 12, 2024.

[8] Z. Lian, L. Sun, H. Sun, K. Chen, Z. Wen, H. Gu, B. Liu, and J. Tao, "Gpt-4v with emotion: A zero-shot benchmark for generalized emotion recognition," *Information Fusion*, vol. 108, p. 102367, 2024.

[9] G. Team, R. Anil, S. Borgeaud, J.-B. Alayrac, J. Yu, R. Soricut, J. Schalkwyk, A. M. Dai, A. Hauth, K. Millican *et al.*, "Gemini: a family of highly capable multimodal models," *arXiv preprint arXiv:2312.11805*, 2023.

[10] J. Bai, S. Bai, S. Yang, S. Wang, S. Tan, P. Wang, J. Lin, C. Zhou, and J. Zhou, "Qwen-vl: A versatile vision-language model for understanding, localization, text reading, and beyond," 2023. [Online]. Available: <https://arxiv.org/abs/2308.12966>

[11] Y. Li, A. Dao, W. Bao, Z. Tan, T. Chen, H. Liu, and Y. Kong, "Facial affective behavior analysis with instruction tuning," in *European Conference on Computer Vision*. Springer, 2024, pp. 165–186.

[12] E. J. Hu, Y. Shen, P. Wallis, Z. Allen-Zhu, Y. Li, S. Wang, L. Wang, W. Chen *et al.*, "Lora: Low-rank adaptation of large language models," *ICLR*, vol. 1, no. 2, p. 3, 2022.

[13] Z. Cheng, Z.-Q. Cheng, J.-Y. He, K. Wang, Y. Lin, Z. Lian, X. Peng, and A. Hauptmann, "Emotion-llama: Multimodal emotion recognition and reasoning with instruction tuning," *Advances in Neural Information Processing Systems*, vol. 37, pp. 110 805–110 853, 2024.

[14] B. Xing, Z. Yu, X. Liu, K. Yuan, Q. Ye, W. Xie, H. Yue, J. Yang, and H. Kälviäinen, "Emo-llama: Enhancing facial emotion understanding with instruction tuning," *arXiv preprint arXiv:2408.11424*, 2024.

[15] S. Bai, K. Chen, X. Liu, J. Wang, W. Ge, S. Song, K. Dang, P. Wang, S. Wang, J. Tang *et al.*, "Qwen2. 5-vl technical report," *arXiv preprint arXiv:2502.13923*, 2025.

[16] T. Pfister, X. Li, G. Zhao, and M. Pietikäinen, "Recognising spontaneous facial micro-expressions," in *2011 international conference on computer vision*. IEEE, 2011, pp. 1449–1456.

[17] S. Polikovsky, Y. Kameda, and Y. Ohta, "Facial micro-expressions recognition using high speed camera and 3d-gradient descriptor," in *3rd international conference on imaging for crime detection and prevention (ICDP 2009)*. IET, 2009, pp. 1–6.

[18] Y.-J. Liu, J.-K. Zhang, W.-J. Yan, S.-J. Wang, G. Zhao, and X. Fu, "A main directional mean optical flow feature for spontaneous micro-expression recognition," *IEEE Transactions on Affective Computing*, vol. 7, no. 4, pp. 299–310, 2015.

[19] S.-T. Liang, J. See, K. Wong, and R. C.-W. Phan, "Less is more: Micro-expression recognition from video using apex frame," *Signal Processing: Image Communication*, vol. 62, pp. 82–92, 2018.

[20] C. Cortes and V. Vapnik, "Support-vector networks," *Machine learning*, vol. 20, pp. 273–297, 1995.

[21] S. Zhao, H. Tao, Y. Zhang, T. Xu, K. Zhang, Z. Hao, and E. Chen, "A two-stage 3d cnn based learning method for spontaneous micro-expression recognition," *Neurocomputing*, vol. 448, pp. 276–289, 2021.

[22] S. Thuseethan, S. Rajasegarar, and J. Yearwood, "Deep3dcnn: A deep 3dcnn-ann framework for spontaneous micro-expression recognition," *Information Sciences*, vol. 630, pp. 341–355, 2023.

[23] A. J. R. Kumar and B. Bhanu, "Micro-expression classification based on landmark relations with graph attention convolutional network," in *Proceedings of the IEEE/CVF conference on computer vision and pattern recognition*, 2021, pp. 1511–1520.

[24] Y. Zhang, H. Wang, Y. Xu, X. Mao, T. Xu, S. Zhao, and E. Chen, "Adaptive graph attention network with temporal fusion for micro-expressions recognition," in *2023 IEEE International Conference on Multimedia and Expo (ICME)*. IEEE, 2023, pp. 1391–1396.

[25] F. Wang, J. Li, C. Qi, L. Wang, and P. Wang, "Jgulf: Joint global and unilateral local feature network for micro-expression recognition," *Image and Vision Computing*, vol. 147, p. 105091, 2024.

[26] Z. Zhai, J. Zhao, C. Long, W. Xu, S. He, and H. Zhao, "Feature representation learning with adaptive displacement generation and transformer fusion for micro-expression recognition," in *Proceedings of the IEEE/CVF Conference on Computer Vision and Pattern Recognition*, 2023, pp. 22 086–22 095.

[27] X.-B. Nguyen, C. N. Duong, X. Li, S. Gauch, H.-S. Seo, and K. Luu, "Micron-bert: Bert-based facial micro-expression recognition," in *Proceedings of the IEEE/CVF Conference on Computer Vision and Pattern Recognition*, 2023, pp. 1482–1492.

[28] S. Zhao, H. Tang, S. Liu, Y. Zhang, H. Wang, T. Xu, E. Chen, and C. Guan, "Me-plan: A deep prototypical learning with local attention network for dynamic micro-expression recognition," *Neural networks*, vol. 153, pp. 427–443, 2022.

[29] S.-T. Liang, Y. S. Gan, J. See, H.-Q. Khor, and Y.-C. Huang, "Shallow triple stream three-dimensional cnn (ststnet) for micro-expression recognition," in *2019 14th IEEE international conference on automatic face & gesture recognition (FG 2019)*. IEEE, 2019, pp. 1–5.

[30] H. Zhou, S. Huang, and Y. Xu, "Incepitr: micro-expression recognition integrating inception-cbam and vision transformer," *Multimedia Systems*, vol. 29, no. 6, pp. 3863–3876, 2023.

[31] G. Wang, S. Huang, and Z. Tao, "Shallow multi-branch attention convolutional neural network for micro-expression recognition," *Multimedia Systems*, vol. 29, no. 4, pp. 1967–1980, 2023.

[32] Z. Wang, K. Zhang, W. Luo, and R. Sankaranarayana, "Htnet for micro-expression recognition," *Neurocomputing*, vol. 602, p. 128196, 2024.

[33] T. Wang and L. Shang, "Temporal augmented contrastive learning for micro-expression recognition," *Pattern Recognition Letters*, vol. 167, pp. 122–131, 2023.

[34] X. Fan, X. Chen, M. Jiang, A. R. Shahid, and H. Yan, "Selfme: Self-supervised motion learning for micro-expression recognition," in *Proceedings of the IEEE/CVF Conference on Computer Vision and Pattern Recognition*, 2023, pp. 13 834–13 843.

[35] Y. Bao, C. Wu, P. Zhang, C. Shan, Y. Qi, and X. Ben, "Boosting micro-expression recognition via self-expression reconstruction and memory contrastive learning," *IEEE Transactions on Affective Computing*, 2024.

[36] S. Liu, X. Mao, S. Zhao, C. Fu, Y. Yu, T. Xu, and E. Chen, "Tgmae: Self-supervised micro-expression recognition with temporal gaussian masked autoencoder," in *2024 IEEE International Conference on Multimedia and Expo (ICME)*. IEEE, 2024, pp. 1–6.

[37] X. Dong, P. Zhang, Y. Zang, Y. Cao, B. Wang, L. Ouyang, S. Zhang, H. Duan, W. Zhang, Y. Li *et al.*, "Internlm-xcomposer2-4khd: A pioneering large vision-language model handling resolutions from 336 pixels to 4k hd," *Advances in Neural Information Processing Systems*, vol. 37, pp. 42 566–42 592, 2024.

[38] J. Zhu, W. Wang, Z. Chen, Z. Liu, S. Ye, L. Gu, Y. Duan, H. Tian, W. Su, J. Shao *et al.*, "Internlml3: Exploring advanced training and test-time recipes for open-source multimodal models," *arXiv preprint arXiv:2504.10479*, 2025.

[39] K. Team, A. Du, B. Yin, B. Xing, B. Qu, B. Wang, C. Chen, C. Zhang, C. Du, C. Wei *et al.*, "Kimi-vl technical report," *arXiv preprint arXiv:2504.07491*, 2025.

[40] K. Chen, Z. Zhang, W. Zeng, R. Zhang, F. Zhu, and R. Zhao, "Shikra: Unleashing multimodal llm's referential dialogue magic," *arXiv preprint arXiv:2306.15195*, 2023.

[41] X. Lai, Z. Tian, Y. Chen, Y. Li, Y. Yuan, S. Liu, and J. Jia, "Lisa: Reasoning segmentation via large language model," in *Proceedings of the IEEE/CVF Conference on Computer Vision and Pattern Recognition*, 2024, pp. 9579–9589.

[42] L. Zhou, Q. Mao, X. Huang, F. Zhang, and Z. Zhang, "Feature refinement: An expression-specific feature learning and fusion method for micro-expression recognition," *Pattern Recognition*, vol. 122, p. 108275, 2022.

[43] S. Zhao, H. Tang, X. Mao, and S. Liu, "Dynamic micro-expression automatic recognition challenge on the fourth chinese conference on affective computing," <https://mea-lab-421.github.io/CCAC-page/>, Jul. 2024, accessed: 2025-04-26.

[44] Z. Liu, K. Yang, Q. Xie, T. Zhang, and S. Ananiadou, "Emollms: A series of emotional large language models and annotation tools for comprehensive affective analysis," in *Proceedings of the 30th ACM SIGKDD Conference on Knowledge Discovery and Data Mining*, 2024, pp. 5487–5496.

[45] X. Lan, J. Xue, J. Qi, D. Jiang, K. Lu, and T.-S. Chua, "Expllm: Towards chain of thought for facial expression recognition," *arXiv preprint arXiv:2409.02828*, 2024.

[46] S. Zhao, H. Tang, X. Mao, S. Liu, Y. Zhang, H. Wang, T. Xu, and E. Chen, "Dfme: A new benchmark for dynamic facial micro-expression recognition," *IEEE Transactions on Affective Computing*, vol. 15, no. 3, pp. 1371–1386, 2023.

[47] W.-J. Yan, X. Li, S.-J. Wang, G. Zhao, Y.-J. Liu, Y.-H. Chen, and X. Fu, "Casme ii: An improved spontaneous micro-expression database and the baseline evaluation," *PloS one*, vol. 9, no. 1, p. e86041, 2014.

[48] J. Li, Z. Dong, S. Lu, S.-J. Wang, W.-J. Yan, Y. Ma, Y. Liu, C. Huang, and X. Fu, "Cas (me) 3: A third generation facial spontaneous micro-expression database with depth information and high ecological validity," *IEEE Transactions on Pattern Analysis and Machine Intelligence*, vol. 45, no. 3, pp. 2782–2800, 2022.